A CD2-Green Fluorescence Protein-Transgenic Mouse Reveals Very Late Antigen-4-Dependent CD8$^+$ Lymphocyte Rolling in Inflamed Venules[1]

Kai Singbartl,[2]*† Jayant Thatte,[2]* Michael L. Smith,* Klaus Wethmar,* Kathy Day,‡ and Klaus Ley[3]*‡

Intravital microscopy allows detailed analysis of leukocyte trafficking in vivo, but fails to identify the nature of leukocytes investigated. Here, we describe the development of a CD2-enhanced green fluorescence protein (EGFP)-transgenic mouse to characterize lymphocyte trafficking during inflammation in vivo. A CD2-EGFP plasmid construct including the CD2 promoter, the EGFP transgene, and the CD2 locus control region was injected into B6CBA/F_1 pronuclei. EGFP$^+$ offspring were backcrossed into C57BL/6 mice for six generations. Flow cytometry demonstrated that all peripheral blood EGFP$^+$ cells were positive for CD2 and negative for the granulocyte Ag Ly 6-G (GR-1). EGFP^{high} cells stained positive for CD2, CD3, CD8, TCR β-chain, and NK1.1 but did not express the B cell and monocyte markers CD45RA, CD19, and CD11b. In vitro stimulation assays revealed no difference in lymphocyte proliferation and IL-2 secretion between EGFP$^+$ and EGFP$^-$ mice. Intravital microscopy of untreated or TNF-α-treated cremaster muscle venules showed EGFP$^+$ cells in vivo, but these cells did not roll or adhere to the vessel wall. In cremaster muscle venules treated with both TNF-α and IFN-γ, EGFP^{high} cells rolled, adhered, and transmigrated at a rolling velocity slightly higher (11 μm/s) than that of neutrophils (10 μm/s). Blocking α_4 integrin with a mAb increased rolling velocity to 24 μm/s. These findings show that CD8$^+$ T cells roll in TNF-α/IFN-γ-pretreated vessels in vivo via an α_4 integrin-dependent pathway. ***The Journal of Immunology*****, 2001, 166: 7520–7526.**

T cells play a central role in immune responses to pathogens and in autoimmune disease (1, 2). Ag recognition by a T cell in the context of an appropriate MHC molecule on the surface of an APC leads to T cell activation and clonal expansion. Recruitment of Ag-specific T cells to sites of inflammation requires extravasation of these cells from the blood across the endothelial barrier into the inflamed tissue. Selectin and integrin adhesion molecules expressed on the surface of lymphocytes and endothelial cells (ECs)[4] as well as chemokines and their receptors are thought to play an important role in effector lymphocyte-EC interactions (3, 4), but no such interaction has ever been observed in vivo.

The cellular and molecular mechanisms governing lymphocyte migration have been investigated in vitro for lymphocyte rolling and adhesion to plate-bound adhesion molecules or to tissue sections (5, 6). These assays have been extremely useful in defining adhesion molecules and their receptors. In vivo, cellular trafficking has been addressed using radiolabeled lymphocytes derived from the skin and the gut (7, 8).

Although the molecular mechanisms underlying the trafficking of naive lymphocytes to peripheral lymph nodes and Peyer's patches has been studied in great detail (4, 9, 10), little is known about how CD8$^+$ T cells get access to inflamed tissues. Based on evidence from homing of CD8$^+$ T cell clones to the lung (11), islets of Langerhans (12), internal elastic lamina and lamina propria of the gut (13), and other inflamed tissues, it is clear that lymphocyte activation is required for recruitment of effector T cells. The sequence of events required is thought to encompass rolling, activation, arrest, and transmigration, akin to the paradigm known for neutrophil recruitment (10). However, it has not been possible to directly demonstrate the adhesion cascade for CD8$^+$ effector T cells in vivo, nor is the adhesion molecule usage in different steps known.

In contrast to neutrophils, most lymphocytes express significant amounts of α_4 integrins, including $\alpha_4\beta_1$ (very late Ag-4, VLA-4) and $\alpha_4\beta_7$ (14). VLA-4 has been shown to mediate lymphocyte rolling (15, 16) and can be rapidly activated, which leads to enhanced adhesiveness (17). Beyond its role in lymphocyte trafficking, VLA-4 is important in the recruitment of monocytes (18), eosinophils (19), and hemopoietic progenitor cells (20). The avidity regulation of VLA-4 can be triggered by tethered chemokines binding to their receptors (17), but the molecular signaling mechanisms underlying increased α_4 integrin avidity are not known.

Direct observation of cellular movement in the microvasculature in real time has become possible using intravital microscopy (21). This technique has permitted analysis of leukocyte-EC interactions that occur before a leukocyte can extravasate from the circulation into the tissue (22, 23). One limitation of this technique is its inability to identify individual cell types under observation, with the exception of one report identifying rolling neutrophils (24).

*Department of Biomedical Engineering, University of Virginia Health Sciences Center, Charlottesville, VA 22908; †Klinik und Poliklinik für Anästhesiologie und operative Intensivmedizin, Westf. Wilhelms-Universität Münster, Münster, Germany; and ‡Cardiovascular Research Center, University of Virginia Health Sciences Center, Charlottesville, VA 22908

Received for publication November 30, 2000. Accepted for publication April 10, 2000.

The costs of publication of this article were defrayed in part by the payment of page charges. This article must therefore be hereby marked *advertisement* in accordance with 18 U.S.C. Section 1734 solely to indicate this fact.

[1] This work was supported by National Institutes of Health Grant HL-64381 and a pilot grant of the Cardiovascular Research Center at the University of Virginia.

[2] K.S. and J.T. contributed equally to this work.

[3] Address correspondence and reprint request to Dr. Klaus Ley, Department of Biomedical Engineering, Box 800709, University of Virginia, Charlottesville, VA 22908. E-mail address: klausley@virginia.edu

[4] Abbreviations used in this paper: EC, endothelial cell; VLA-4, very late Ag-4; GFP, green fluorescence protein; EGFP, enhanced GFP.

 0022-1767/01/$02.00

This limits assessment of cellular interaction of a specific cell type with the endothelium. Recently, a CD4-green fluorescence protein (GFP)-transgenic mouse has been described to study $CD8^+$ T cell differentiation in vivo (25). However, activated T cells lose GFP expression in the CD4-GFP mouse, making it less suitable for in vivo studies of effector T cell trafficking. Here, we describe the development of a transgenic mouse expressing enhanced GFP (EGFP) in T cells under a CD2 promoter with GFP expression even in activated T cells. We demonstrate that this mouse is a useful research tool for selective analysis of T cell rolling and adhesion during inflammation in vivo.

Materials and Methods

Transgenic construct and microinjection

An *Eco*RI/*Not*I (blunted) fragment of pEGFP-N1 (Clontech, Palo Alto, CA) was cloned into the *Eco*RI/*Sma*I sites between the human CD2 promoter and the CD2 locus control region of the pBS CD2 construct (26). The construct (see Fig. 1) was tested for GFP expression in transient transfection of cultured Jurkat cells. The construct was then prepared for pronuclear injection into fertilized $B6CBA/F_1$ eggs by removing the plasmid backbone by a *Kpn*I/*Not*I digestion and subsequent agarose gel purification. Transgenic mice were generated using standard microinjection techniques at the University of Virginia Transgenic Mouse Core Facility (Charlottesville, VA). Tail DNA was analyzed for the transgene by PCR, and tail bleeds from transgene positive mice were analyzed for GFP expression by flow cytometry. Founder animals were backcrossed into C57BL/6J wild-type mice for six generations and maintained at the University of Virginia Center for Comparative Medicine. Mice were used between 7 and 12 wk of age. $EGFP^-$ littermates served as controls. All experiments were conducted according to protocols approved by the University of Virginia Institutional Animal Care and Use Committee.

Surface Ag staining and flow cytometry

To characterize surface Ag expression of $EGFP^+$ cells, peripheral blood leukocytes, lymph node cells, and splenocytes from $EGFP^+$ mice were labeled with PE-conjugated anti-mouse Abs (all obtained from BD Phar Mingen, San Diego, CA): anti-CD2 (clone RM2-5), anti-CD4 (clone RM4-5), anti-CD8α (clone 53-6.7), anti-CD8β (clone 53-5.8), anti-CD3 (clone 17A2), anti-TCR-β (clone H57-597), anti-NK1.1 (clone PK136), anti-CD45RA/B220 (clone RA3-6B2), anti-CD19 (clone 1D3), anti-CD11b (clone M1/70), anti-Ly-6G (clone RB6-8C5). After RBC lysis with a 1.5 M NH_4Cl solution, all samples were run on a FACScan flow cytometer (BD Biosciences, San Jose, CA). Data analysis was performed using CellQuest software (BD Biosciences). Activated splenocytes were labeled with PE-conjugated anti-mouse Abs to activation markers CD25 (clone M-A251), CD69 (clone FN50), and CD44 (clone C26) and analyzed as described above.

T cell proliferation and IL-2 assays

Splenocytes were plated at 4×10^5 cells per well in 96-well flat-bottom plates after RBC lysis and were stimulated with graded doses of Con A (Sigma, St. Louis, MO), anti-CD3ϵ Ab clone 145-2C11 (BD PharMingen), or with 10 ng/ml PMA (Sigma) plus 500 ng/ml ionomycin (Sigma) for 48 h. Controls were run in parallel without any stimulation. Plates were pulsed with 1 μCi of ^3H per well for the last 12 h of the assay, and thymidine incorporation was analyzed by liquid scintillation spectroscopy (LKB Pharmacia, Uppsala, Sweden). Data are expressed as mean values of triplicate measurements $\pm$ SD. For the IL-2 assay, culture supernatants were harvested 24 h poststimulation, and IL-2 levels in the supernatant were estimated using an IL-2 ELISA kit (BD PharMingen) as per manufacturer's instructions.

Intravital microscopy

Before surgery, mice were injected with an intrascrotal injection of 250 ng murine rTNF-α (Genzyme, Cambridge, MA) for 3–6 h, 2.5 μg murine rIFN-γ (Sigma) for 6 h, and 10 U hirudin (Sigma) in 220 μl isotonic saline. Mice were anesthetized with i.p. injections of ketamine (125 μg/g body weight; Ketalar; Parke-Davis, Morris Plains, NJ), xylazine (12.5 μg/g body weight; Phoenix Scientific, St. Joseph, MO), and atropine sulfate (0.025 μg/g body weight; Elkins-Sinn, Cherry Hill, NJ), placed on a heating pad to maintain body temperature, and prepared for intravital microscopy (27). The cremaster muscle was prepared as described and superfused with thermocontrolled (35°C) HCO_3-buffered saline (22). Microscopy of the cremaster muscle was performed using an intravital microscope (Axioskop; Carl Zeiss, Thornwood, NY) with a $\times$40 saline immersion objective (SW 40/0.75). Vessels to be analyzed were chosen on the basis of video image clarity and resolution. Using stroboscopic (30 flashes/s) epifluorescence, intravital microscopy allowed for a clear differentiation between $EGFP^{high}$ and $EGFP^{low}$ cells (see Fig. 2). Vessels were recorded on videotape (S-VHS recorder; Panasonic, Osaka, Japan) with a SIT camera (SIT 66; DAGE-MTI, Michigan City, IN). Mean blood flow velocity, based on centerline RBC velocity (Circusoft; www.circusoft.com), and wall shear rates were calculated as described elsewhere (28). The flux fraction of $EGFP^{high}$ cells was calculated by dividing the counted number of $EGFP^{high}$ cells passing a line perpendicular to the vessel by the total leukocyte (white blood cell) flux in the same vessel.

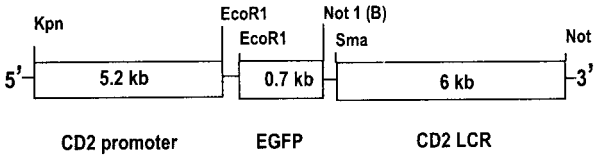

FIGURE 1. Restriction map of the CD2-EGFP DNA construct used for microinjection. The GFP coding sequence was placed under transcriptional control of the human CD2 promoter. The vector backbone was excised and the construct was injected into $B6CBAF_1/J\ F_2$ embryos. LCR, Locus control region.

Rolling velocity

Rolling velocities of single leukocytes along a venule segment were determined for several leukocytes in postcapillary venules (diameter 30–90 μm). All leukocyte displacements and velocities were measured on a Macintosh computer (Apple Computer, Cupertino, CA) using the public domain NIH Image program (developed at the National Institutes of Health

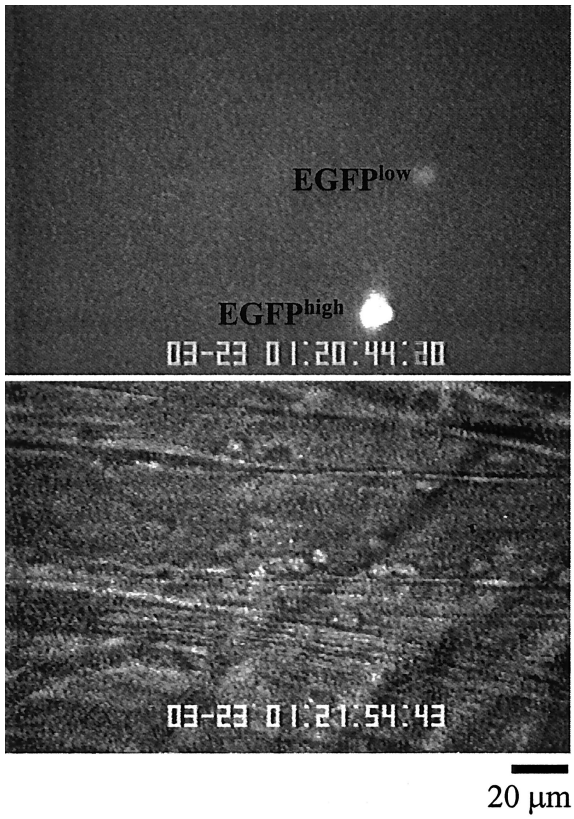

FIGURE 2. Visualization of GFP^+ cells by intravital microscopy. *Upper panel* shows an epifluorescent image of a cell expressing high levels of GFP ($EGFP^{high}$) and one expressing lower level of GFP ($EGFP^{low}$). *Lower panel* shows the transillumination image of the same postcapillary venule of the inflamed cremaster muscle.

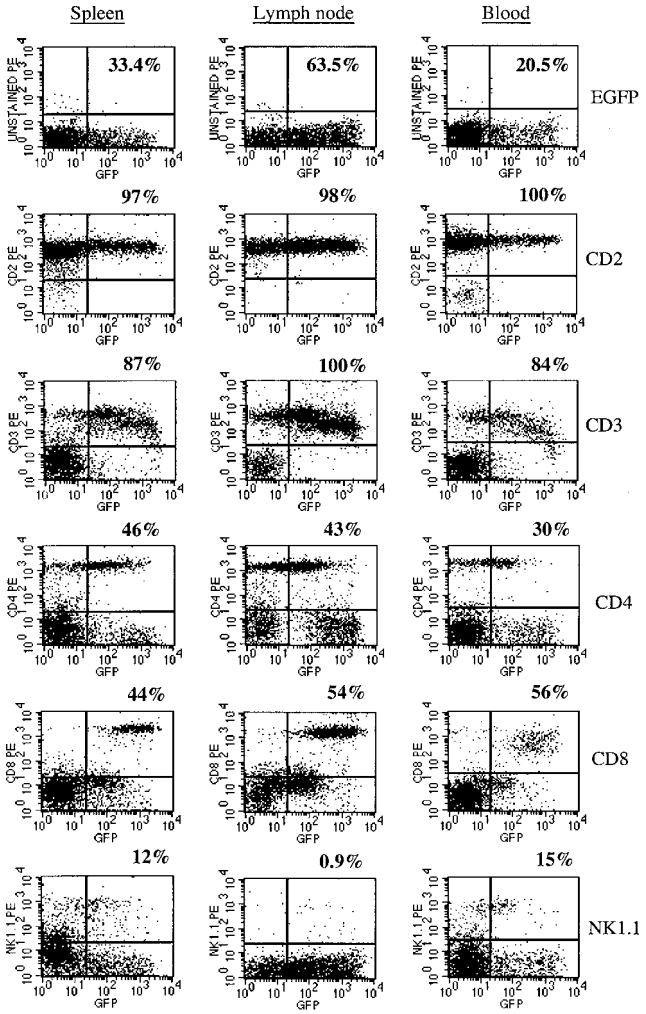

FIGURE 3. Characterization of EGFP$^+$ leukocytes in the spleen (*left*), lymph node (*middle*), and peripheral blood (*right*). Cells from each tissue were stained with PE-conjugated Abs to the indicated cell surface markers and analyzed by flow cytometry. A total of 33.4% of splenocytes, 63.5% of lymph node cells, and 20.5% of peripheral blood leukocytes were positive for EGFP. The percentage indicated above each plot represents the percentage of EGFP$^+$ cells expressing each marker (CD2, CD3, CD4, CD8, and NK1.1).

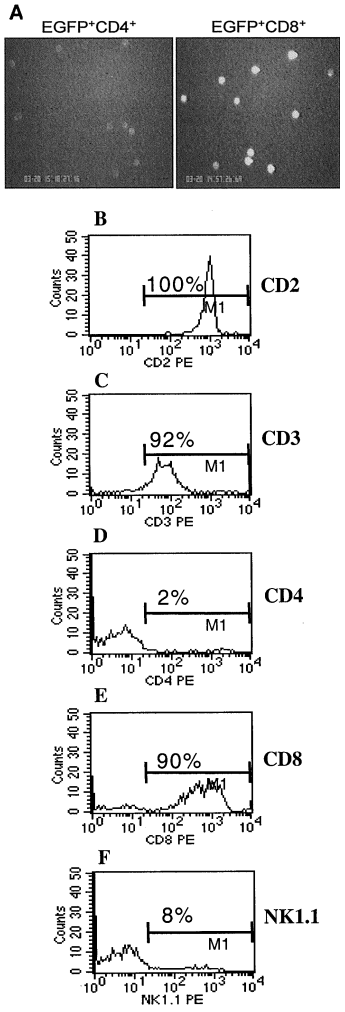

FIGURE 4. *A*, Visualization of EGFP$^+$ peripheral blood CD4 and CD8 T cells by epifluorescence microscopy. Cells were stained with PE-conjugated Abs to CD4 or CD8, and EGFP$^+$ CD4 and CD8 T cells were sorted and observed under an epifluorescent microscope. *B–F*, Analysis of the brightest 1% of total peripheral blood leukocytes. Cells were gated for brightest 1% of the peripheral blood leukocytes and analyzed for cell surface expression of indicated markers by flow cytometry. The percentage indicates the percentage of EGFP$^+$ cells expressing each marker.

and available on the internet at http://rsb.info.nih.gov/nih-image/). The rolling velocity was calculated as displacement in micrometers per second.

Adhesion molecule blocking experiments

Individual rolling EGFP^{high} cells were tracked from the time entering a large postcapillary venule (diameter >50 μm) until the cells were lost. Displacements of tracked EGFP^{high} cells were measured offline every tenth frame for the entire observation period. After tracking two to four EGFP^{high} cells per vessel observed, animals were injected with 30 μg mAb PS/2 directed against murine α_4 integrin intra-arterially; 10 min later, the tracking experiments were continued studying one to four EGFP^{high} cells in the same vessel. In separate experiments, P-selectin mAb RB40.34 (a gift from D. Vestweber, Münster, Germany), E-selectin mAb 9A9 (a gift from B. Wolitzky, Hoffman-La Roche, Nutley, NJ), L-selectin mAb MEL-14 (American Type Culture Collection, Manassas, VA), or CD44 mAb KM81 (American Type Culture Collection) were injected at 30 μg/mouse i.v. Blood samples for white blood cell counts were taken immediately before and 5 min after Ab injection.

Data analysis

All data are given as mean ± SEM. Statistical analysis was performed using Student's *t* test, Mann-Whitney rank sum test, and ANOVA on ranks test. Differences were considered statistically significant if $p < 0.05$.

Results

Generation of CD2-EGFP$^+$-transgenic mice

To generate CD2-EGFP$^+$-transgenic mice, the EGFP coding sequence was placed under control of the human CD2 promoter and locus control region (Fig. 1). This strategy has been shown to result in a position-independent, copy number-dependent T cell-specific expression of the desired gene product (26). Microinjection of the construct into B6CBA/F_1 fertilized eggs resulted in two positive founders, identified by PCR, tail bleeding, and subsequent flow cytometry. These mice were backcrossed into C57BL/6 wild-type mice. Whereas offspring from one founder lost EGFP expression past N3, offspring from founder two revealed a stable EGFP expression throughout (N7 today).

In vivo visualization of EGFP$^+$ cells

Using intravital microscopy of the cremaster muscle, we sought to visualize EGFP$^+$ cell trafficking in vivo. However, in two well-known models of inflammation in the cremaster muscle, with or without TNF-α pretreatment (22), no or only short, transient interactions between EGFP$^+$ cells and the endothelium could be

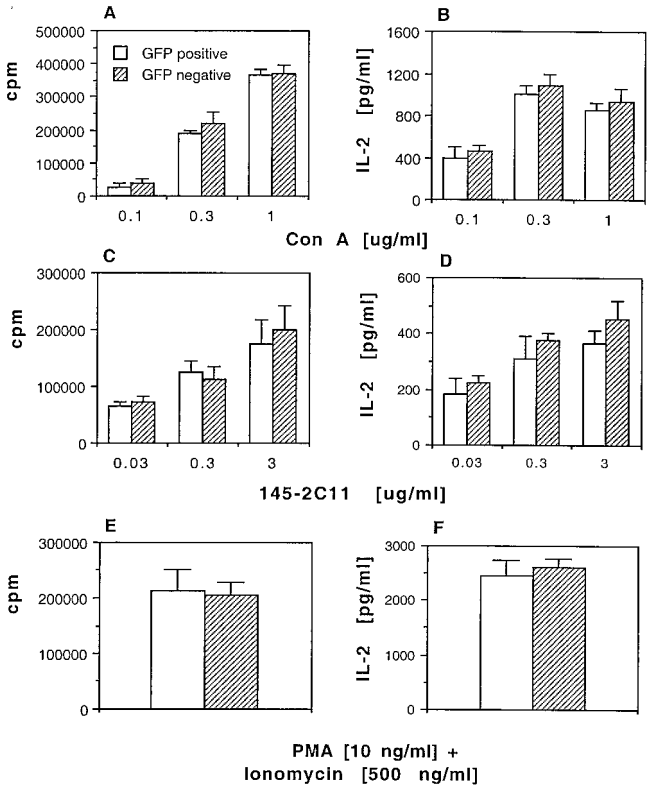

FIGURE 5. Splenocyte proliferative response (*A*, *C*, and *E*) to stimulation by mitogen, Ab-mediated cross-linking, or PMA and ionomycin. A total of 4×10^5 splenocytes were cocultured with graded doses of Con A (*A*), anti-CD3ϵ Ab, 145-2C11 (*C*), or 10 ng/ml PMA plus 500 ng/ml ionomycin (*E*). Data are expressed as mean of triplicates ± SD. Background ^{3}H incorporation in the absence of stimulus was <1000 cpm for all cultures. *B*, *D*, and *F*, IL-2 production. Culture supernatants were harvested at 24-hours poststimulation and analyzed for IL-2 activity by ELISA in response to Con A (*B*), anti-CD3ϵ (*D*), or PMA plus ionomycin (*F*).

observed. No stable rolling of EGFP$^+$ cells was seen in either model. Because pretreatment of ECs with both TNF-α and IFN-γ has been shown to lead to firm adhesion of activated T lymphocytes in vitro (29), cremaster muscles were pretreated with a combination of TNF-α for 3–6 h and IFN-γ for 6 h. This resulted in stable of EGFP$^+$ cells rolling at a median velocity similar to that of neutrophils (11 μm/s), as well as occasional adhesion and transmigration. Intravital microscopy was able to distinguish between EGFP^{high} and EGFP^{low} cells (Fig. 2). EGFP^{high} cells accounted for 0.7% of all leukocytes.

Surface Ag expression of EGFP$^+$ cells

Analysis of EGFP expression in splenocytes, peripheral lymph node cells, and leukocytes in peripheral blood shows 33.4, 63.5, and 20.5% of cells positive for EGFP in the spleen, lymph node, and peripheral blood, respectively (Fig. 3). Ninety-seven to 100% of all EGFP$^+$ cells express CD2. Both CD4 as well as CD8 T cells in all three tissues express EGFP. CD4 T cells are predominantly EGFP^{low}, whereas CD8 T cells are EGFP^{high}. Between 0.9 and 15% of EGFP^{low} cells express NK1.1 in these tissues (Fig. 3). B cells, macrophages, and granulocytes do not express EGFP (data not shown). Because intravital microscopy uses an epifluorescent microscope to visualize cells, we looked at the intensity of EGFP in these two T cell subsets under the epifluorescent microscope after sorting the EGFP^{low} CD4 T cells and EGFP^{high} CD8 T cells. Clearly, CD4 T cells show very poor fluorescence, whereas CD8 T cells appear to be very bright (Fig. 4*A*).

EGFP^{high} cells in peripheral blood accounted for ~0.7% of all leukocytes as determined by intravital microscopy. The brightest 1.0% of all analyzed cells were CD2$^+$, 90% of the EGFP^{high} cells were CD8 T cells, 2.5% were CD4 T cells, and 8% stained positive for the NK1.1 marker (Fig. 4*B*). These findings identify peripheral blood EGFP^{high} cells in our EGFP-transgenic mouse as predominantly CD8$^+$ lymphocytes.

In vitro stimulation and proliferation assays

Stimulation of splenocytes from EGFP$^+$ and EGFP$^-$ mice with anti-CD3ϵ Ab, Con A, or PMA showed similar rates of proliferation (Fig. 5, *A*, *C*, and *E*) and IL-2 secretion (Fig. 5, *B*, *D*, and *F*). These data suggest that the transgene did not impair lymphocyte function.

Upon stimulation with an anti-CD3 Ab, all EGFP$^+$ cells expressed cell surface activation markers CD25, CD69, and increased levels of CD44 on day 3 and 7 postactivation (Fig. 6). In

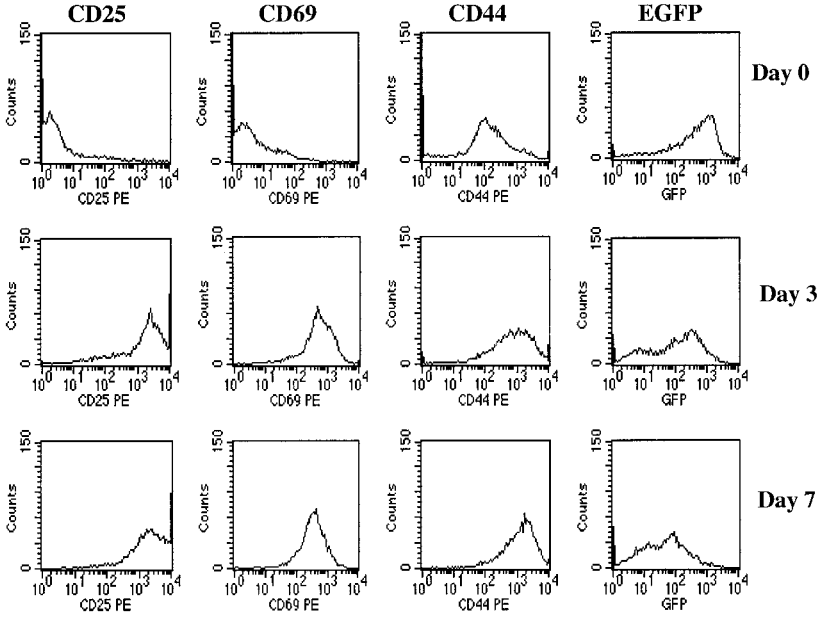

FIGURE 6. Expression of EGFP in activated T cells. Splenocytes were stimulated with 10 μg/ml anti-CD3ϵ Ab,145-2C11, and 10U/ml rIL-2 and analyzed for expression of cell surface activation markers CD25, CD69, and CD44 by flow cytometry on days 0, 3, and 7. For EGFP expression, CD8$^+$ T cells were gated and 10,000 events were collected for each time point. Day 0 represents analysis before activation.

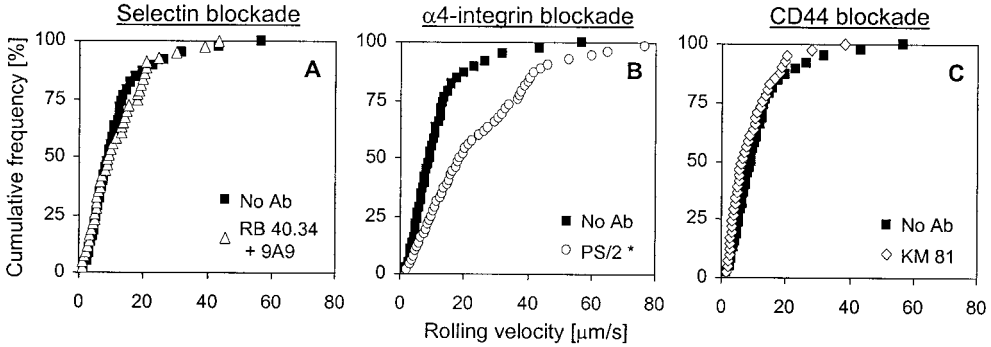

FIGURE 7. Cumulative frequencies for rolling velocities of EGFP^{high} cells before (no Ab) and after treatment with 30 μg of (*A*) P-selectin Ab RB40.34 and E-selectin Ab 9A9, (*B*) α_4 integrin Ab PS/2, and (*C*) CD44 Ab KM81 in postcapillary venules of inflamed cremaster muscle. The average velocity for no Ab treatment is 11.3 μm/s, after RB40.34 plus 9A9 is 11.8 μm/s, after PS/2 is 24.4 μm/s, and after KM81 is 8.9 μm/s. *, Significantly different ($p < 0.05$) from no Ab treatment.

a previously reported GFP-transgenic mouse (25), anti-CD3 Ab-activated CD8$^+$ T cells showed loss of GFP expression by day 7. In our mice, the activated CD8$^+$ T cells continued to express EGFP, albeit at lower levels, even on day 7 (Fig. 6), thereby indicating that EGFP expression is not lost postactivation.

Involvement of α_4 integrin in CD8$^+$ T cell rolling

To address the molecular mechanisms of rolling of CD8$^+$ T cells in inflamed venules in vivo, we blocked several endothelial and leukocyte adhesion molecules using mAbs. Injection of blocking concentrations of Abs to P-selectin, E-selectin, or L-selectin failed to alter the rolling velocities of EGFP^{high} cells (Fig. 7*A* and data not shown) as well as total leukocytes in the transgene-negative littermate controls (Fig. 8*A*). Although the rolling velocities did not change after blocking P- or E-selectin, the rolling flux fraction was altered significantly after blocking both P- and E-selectin in the transgene-negative littermate controls (Fig. 8*B*). After injection of the α_4 integrin mAb PS/2, the average rolling velocity of EGFP$^+$ cells was significantly elevated from 11 to 24 μm/s (Fig. 7*B* and Table I). This indicates that α_4 integrin is required to stabilize rolling of these CD8$^+$ T cells in inflamed venules in vivo. We also investigated the role of CD44 in CD8 T cell rolling as a candidate other than α_4 integrin. As shown in Fig. 7*C*, CD44 does not contribute to CD8 T cell rolling in our model, as blocking CD44 with an anti-CD44 Ab, KM81, did not alter the rolling velocity. Unknown selectin- and CD44-independent mechanisms prevent EGFP^{high} cells from detaching even when α_4 integrins are blocked.

Discussion

Intravital microscopy is as a powerful tool for real-time analysis of inflammatory cell rolling, adhesion, and migration in vivo (21). However, this technique does not permit identification of individual cell types during observation. Currently, for this purpose, cells are purified in vitro, labeled with fluorescent dyes, and reinjected in the host for analysis. Handling of cells in vitro during the isolation procedure could lead to perturbation of cell surface molecules and change the activation status of a cell (30). To avoid this, it would be desirable to identify cells in vivo, without having to handle them in vitro, before analysis. To address this issue, we generated transgenic mice that express EGFP in T cells for direct observation in vivo.

Using intravital microscopy, it was possible to identify EGFP^{high} and EGFP^{low} cells in the peripheral blood (Fig. 2) of untreated, EGFP-transgenic mice. EGFP^{high} cells are most readily detected by intravital microscopy and accounted for ~0.7% of peripheral blood leukocytes. Ninety percent of these cells are comprised of CD8 T cells, 2% of CD4 T cells, and 8% of NK cells, with no B cells, monocytes, or neutrophils. The fluorescence intensity of EGFP was at least one decade higher in CD8$^+$ T cells compared with CD4$^+$ T cells as analyzed by flow cytometry (Fig.

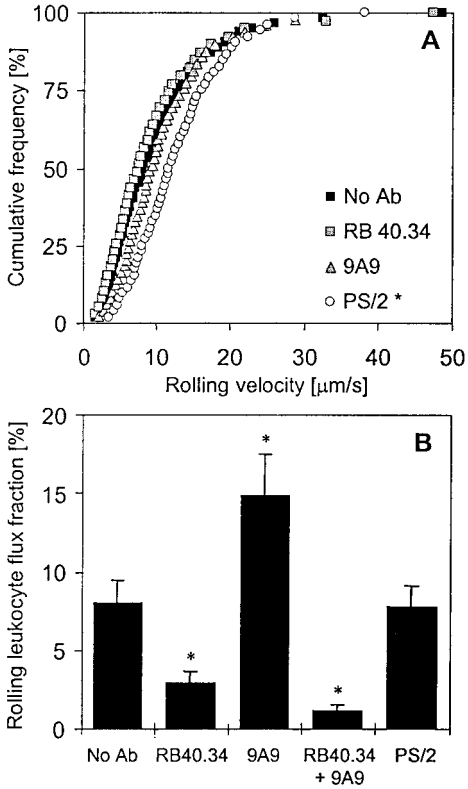

FIGURE 8. *A*, Cumulative frequencies for rolling velocities of all leukocytes before (no Ab) and after treatment with 30 μg of anti-P-selectin Ab RB40.34 and E-selectin Ab 9A9 and α_4 integrin Ab PS/2 in postcapillary venules of TNF-α and IFN-γ-treated cremaster muscle. The average velocity for no Ab treatment is 9.6 μm/s, after RB40.34 is 10.6 μm/s, after 9A9 is 9.2 μm/s, and after PS/2 is 12.8 μm/s. *, Significantly different ($p < 0.05$) from no Ab treatment. *B*, Rolling leukocyte flux fraction in transgene-negative littermates with no Ab treatment (8%) and after treatment with anti-P-selectin Ab RB40.34 (2.9%), E-selectin Ab 9A9 (14.9%), P- and E-selectin Abs (1.2%), and α_4 integrin Ab PS/2 (7.8%) in postcapillary venules of inflamed cremaster muscle. *, Significantly different ($p < 0.05$) from no Ab treatment.

Table I. *Hemodynamic parameters and average rolling velocities for EGFP-transgenic mice and transgene-negative littermates*

	Treatment	Vessels (*n*)	Cells (*n*)	Diameter (μm)	Centerline RBC Velocity (mm/s)	Shear Rate (s^{-1})	Average Rolling Velocity (μm/s)
EGFP^{high} cells	No Ab	10	27	67 ± 5	3.5 ± 0.3	580 ± 60	11.3 ± 0.5
	RB40.34 + 9A9	4	12	69 ± 5	3.3 ± 0.3	510 ± 30	11.8 ± 1.0
	PS/2	7	16	57 ± 5	3.5 ± 0.4	650 ± 70	24.4 ± 1.1*
	KM81	2	8	71 ± 2	2.5 ± 0.3	370 ± 30	8.9 ± 0.6
All leukocytes	No Ab	31	609	41 ± 2	3.5 ± 0.3	900 ± 60	9.6 ± 0.3
	RB 40.34	13	191	43 ± 2	3.9 ± 0.4	950 ± 80	10.6 ± 0.4
	9A9	12	241	36 ± 2	2.2 ± 0.2	620 ± 50	9.2 ± 0.5
	PS/2	13	257	45 ± 3	3.5 ± 0.3	870 ± 100	12.8 ± 0.4*

*, Significantly different ($p < 0.05$) from no Ab treatment.

3) and by epifluorescent microscopy (Fig. 4*A*). Taken together, these data show that almost all EGFP ^{high} cells are CD8 T cells.

Introduction of the transgene did not perturb T cell function, because the T cells from EGFP$^+$ mice were comparable to those from transgene-negative littermates, as assessed by T cell proliferation and IL-2 production. In a previously reported GFP-transgenic mouse (25), anti-CD3 Ab-activated CD8$^+$ T cells showed loss of EGFP expression by day 7. In the transgenic mice reported here, although activation of T cells using an anti-CD3 Ab led to a down-regulation of EGFP expression in CD8$^+$ T cells, the majority of these activated cells (~80%) continue to express EGFP even on day 7 postactivation (Fig. 6).

Recruitment of neutrophils is known to be achieved through a series of well-defined interactions between the neutrophil and EC that encompass rolling, activation, and arrest followed by transmigration (10). Lymphocytes are thought to be recruited through a similar mechanism (31), and a multistep process has clearly been shown for homing of naive lymphocytes to secondary lymphatic organs (4, 32), but not for effector T cells. Selectin and integrin molecules appear to play an important role in migration of T cells to sites of inflammation. E- and P-selectin are involved in CD4$^+$ T cell migration into inflamed skin (33, 34), whereas migration of activated CD8$^+$ T cells to sites of viral infection appears to be selectin independent (35). Integrins like VLA-4, LFA-1, and Mac-1 and their ligands ICAM-1 and VCAM-1 appear to be important for CD8$^+$ T cell recruitment in a lymphocyte choriomeningitis virus infection model (36–39). Another integrin, $\alpha_4\beta_7$, plays an important role in entry of T cells into the lamina propria and Peyer's patches (40). Despite this information, it has not been possible to directly demonstrate the adhesion cascade for CD8$^+$ effector T cells in vivo, nor is the adhesion molecule usage in different steps known.

Using the CD2-EGFP-transgenic mouse, we have begun to address the adhesion cascade for CD8$^+$ T cells in vivo. In the present study, we analyzed the role for P-, E-, and L-selectin, CD44, and VLA-4 in rolling and adhesion of EGFP^{high} T cells to inflamed endothelium in vivo. Blocking P-, E-, or L-selectin alone or in combination did not change the rolling velocities of these cells (Fig. 7*A* and data not shown). Although the CD44 ligand, hyaluronate, is known to be up-regulated by TNF-α treatment (41), blocking CD44 did not alter the rolling velocity (Fig. 7*C*) indicating CD44-independent rolling of EGFP^{high} T cells on the inflamed endothelium in our model. Injection of anti-α_4 Ab increased the rolling velocity of EGFP^{high} cells significantly from 11 to 24 μm/s (Fig. 7*B* and Table I). This 2-fold increase indicates a dependence on α_4 integrin for slow rolling of T cells on inflamed endothelium. Surface expression of α_4 integrin appears to be important in T cell recruitment as the presence of this molecule has been shown to enhance the pathogenicity of T cell clones by virtue of their ability to transmigrate through the endothelium in the experimental autoimmune encephalomyelitis model (42), and the levels of VLA-4 on the cell surface have been correlated to the degree of protection conferred by CD8$^+$ T cell clones in an animal model of malaria (43).

Interestingly, pretreatment with either TNF-α alone or IFN-γ alone failed to induce any stable rolling of the EGFP^{high} cells. Pretreatment with TNF-α alone is sufficient for rolling and arrest of neutrophils (27). In this model, the data suggests that IFN-γ plus TNF-α produces conditions not induced by TNF-α alone. It is possible that IFN-γ-dependent chemokine up-regulation may contribute to CD8 T cell rolling and/or adhesion. For example, IFN-γ alone or in combination with TNF-α is known to up-regulate the CXCR3 ligand IFN-inducible T cell α chemoattractant in human ECs (44). However, the present study does not address the potential role of chemokines.

In conclusion, we use a novel CD2-EGFP-transgenic mouse to show that CD8$^+$ T cells use α_4 integrins to roll on inflamed endothelium in vivo. This mouse will be very useful in elucidating the adhesion cascade involved in recruitment of CD8 T cells to sites of inflammation in vivo.

Acknowledgments

We thank Dr. Lou Hammarskjold for the CD2 construct, Jennifer Bryant and Michele Kirkpatrick for animal husbandry, William Ross for flow cytometry, and Dr. Sonia Pearson-White for microinjections. We also thank Dr. Larry Karns for assistance with transfection assays.

References

1. Scott, P., and S. Kaufmann. 1991. The role of T cell subsets and cytokines in the regulation of infection. *Immunol. Today 12:346.*
2. Moller, G. 1993. Models of autoimmunity. *Immunol. Rev. 118:310.*
3. Salmi, M., and S. Jalkanen. 1997. How do lymphocytes know where to go: current concepts and enigmas of lymphocyte homing. *Adv. Immunol. 64:139.*
4. von Andrian, U. H., and C. R. Mackay. 2000. T-cell function and migration: two sides of the same coin. *N. Engl. J. Med. 343:1020.*
5. Knorr, K., and M. L. Dustin. 1997. The lymphocyte function-associated antigen 1 I domain is a transient binding module for intercellular adhesion molecule (ICAM)-1 and (ICAM)-3 in hydrodynamic flow. *J. Exp. Med. 186:719.*
6. Stamper, H. B., and J. J. Woodruff. 1977. An in vitro model of lymphocyte homing. I. Characterization of the interaction between thoracic duct lymphocytes and specialized high endothelial venules of lymph nodes. *J. Immunol. 119:722.*
7. Issekutz, T. B., W. Chin, and J. B. Hay. 1982. The characterization of lymphocyte migrating through chronically inflamed tissues. *Immunology 46:59.*
8. Guy-Grand, D., C. Griscelli, and P. Vassalli. 1978. The mouse gut T lymphocyte, a novel type of T cell: nature, origin and traffic in mice in normal and graft-versus-host conditions. *J. Exp. Med. 148:1661.*
9. Butcher, E. C., and L. J. Picker. 1996. Lymphocyte homing and homeostasis. *Science 272:60.*
10. Springer, T. A. 1994. Traffic signals for lymphocyte recirculation and leukocyte emigration: the multistep paradigm. *Cell 76:301.*
11. Enelow, R. I., A. Z. Mohammed, M. H. Stoler, A. N. Liu, J. S. Young, Y. H. Lou, and T. J. Braciale. 1998. Structural and functional consequences of alveolar cell recognition by CD8$^+$ T lymphocytes in experimental lung disease. *J. Clin. Invest. 102:1653.*

12. Yoneda, R., K. Yokono, M. Nagata, Y. Tominaga, H. Moriyama, K. Tsukamoto, M. Miki, N. Okamoto, H. Yasuda, K. Amano, and M. Kasuga. 1997. CD8 cytotoxic T-cell clone rapidly transfers autoimmune diabetes in very young NOD and MHC class I-compatible *scid* mice. *Diabetologia 40:1044.*
13. Lefrancois, L., C. M. Parker, S. Olson, W. Muller, N. Wagner, and L. Puddington. 1999. The role of β_7 integrins in CD8 T cell trafficking during an antiviral immune response. *J. Exp. Med. 189:1631.*
14. Holzmann, B., and I. L. Weissman. 1989. Integrin molecules involved in lymphocyte homing to Peyer's patches. *Immunol. Rev. 108:45.*
15. Jones, D. A., L. V. McIntire, C. W. Smith, and L. J. Picker. 1994. A two-step adhesion cascade for T cell/endothelial cell interactions under flow conditions. *J. Clin. Invest. 94:2443.*
16. Ruck, P., J.-C. Xiao, and E. Kaiserling. 1995. Immunoreactivity of sinusoids in hepatocellular carcinoma: an immunohistochemical study using lectin UEA-1 and antibodies against endothelial markers, including CD34. *Arch. Pathol. Lab. Med. 119:173.*
17. Grabovsky, V., S. Feigelson, C. Chen, D. A. Bleijs, A. Peled, G. Cinamon, F. Baleux, F. Arenzana-Seisdedos, T. Lapidot, Y. Van Kooyk, R. R. Lobb, and R. Alon. 2000. Subsecond induction of α_4 integrin clustering by immobilized chemokines stimulates leukocyte tethering and rolling on endothelial vascular cell adhesion molecule 1 under flow conditions. *J. Exp. Med. 192:495.*
18. Huo, Y., A. Hafezi-Moghadam, and K. Ley. 2000. Role of vascular adhesion molecule-1 (VCAM-1) and fibronectin connecting segment-1 (CS-1) in monocyte adherence on early atherosclerotic lesions. *Circ. Res. 87:153.*
19. Lobb, R. R., and M. E. Hemler. 1994. The pathophysiologic role of α_4 integrins in vivo. *J. Clin. Invest. 94:1722.*
20. Papayannopoulou, T., and C. Craddock. 1997. Homing and trafficking of hemopoietic progenitor cells. *Acta Haematologica 97:97.*
21. Menger, M. D., and H. A. Lehr. 1993. Scope and perspectives of intravital microscopy—bridge over from in vitro to in vivo. *Immunol. Today 14:519.*
22. Ley, K., D. C. Bullard, M. L. Arbones, R. Bosse, D. Vestweber, T. F. Tedder, and A. L. Beaudet. 1995. Sequential contribution of L- and P-selectin to leukocyte rolling in vivo. *J. Exp. Med. 181:669.*
23. Kunkel, E. J., C. L. Ramos, D. A. Steeber, W. Muller, N, Wagner, T. F. Tedder, and K. Ley. 1998. The roles of L-selectin, β_7-integrins, and P-selectin in leukocyte rolling and adhesion in high endothelial venules of Peyer's patches. *J. Immunol. 161:2449.*
24. Tangelder, G. J., C. J. J. G. Janssens, D. W. Slaaf, M. G. A. oude Egbrink, and R. S. Reneman. 1995. In vivo differentiation of leukocytes rolling in mesenteric postcapillary venules. *Am. J. Physiol. 268:H909.*
25. Manjunath, N., P. Shankar, B. Stockton, P. D. Dubey, J. Lieberman, and U. H. von Andrian. 1999. A transgenic mouse model to analyze $CD8^+$ effector T cell differentiation in vivo. *Proc. Natl. Acad. Sci. USA 96:13932.*
26. Zhumabekov, T., P. Corbella, P. Tolaini, and D. Kioussis. 1995. Improved version of a human CD2 minigene-based vector for T cell-specific expression in transgenic mice. *J. Immunol. Methods 185:133.*
27. Kunkel, E. J., J. L. Dunne, and K. Ley. 2000. Leukocyte arrest during cytokine-dependent inflammation in vivo. *J. Immunol. 164:3301.*
28. Kunkel, E. J., and K. Ley. 1996. Distinct phenotype of E-selectin deficient mice. E-selectin is required for slow leukocyte rolling in vivo. *Circ. Res. 79:1196.*
29. Piali, L., C. Weber, G, LaRosa, C. R. Mackay, T. A. Springer, I. Clark-Lewis, and B. Moser. 1998. The chemokine receptor CXCR3 mediates rapid shear-resistant adhesion induction of effector T lymphocytes by the chemokines IP10 and Mig. *Eur. J. Immunol. 28:961.*
30. Haslett, C., L. A. Guthrie, M. M. Kopaniak, R. B. Johnston, and P. M. Hensen. 1985. Modulation of multiple neutrophil functions by preparative methods or trace concentrations of bacterial lipopolysaccharide. *Am. J. Pathol. 119:101.*
31. Shimizu, Y., W. Newman, W. Tanaka, and S. Shaw. 1992. Lymphocyte interactions with endothelial cells. *Immunol. Today 13:106.*
32. Bargatze, R. F., M. A. Jutila, and E. C. Butcher. 1995. Distinct roles of L-selectin and integrins $\alpha_4\beta_7$ and LFA-1 in lymphocyte homing to Peyer's patch-HEV in situ: the multi-step model confirmed and refined. *Immunity 3:99.*
33. Tietz, W., Y. Allemand, E. Borges, D. von Laer, R. Hallmann, and D. Vestweber. 1998. CD4 T cells migrate into inflamed skin only if they express ligands for E- and P-selectin. *J. Immunol. 161:963.*
34. Borges, E., W. Tietz, M, Steegmaier, T., Moll, R., Hallmann, and A. Hamann. 1997. P-selectin glycoprotein ligand-1 (PSGL-1) on T helper 1 bout not on T helper 2 cells binds to P-selectin and supports migration into inflamed skin. *J. Exp. Med. 185:573.*
35. Bartholdy, C., O. Marker, and A. R. Thomsen. 2000. Migration of activated CD8 T lymphocytes to sites of viral infection does not require endothelial selectins. *Blood 95:1362.*
36. Christensen, J. P., E. C. Andersson, A. Scheynius, O. Marker, and A. R. Thomsen. 1995. α_4 integrin directs virus-activated CD T cells to sites of infection. *J. Immunol. 154:5293.*
37. Christensen, J. P.,O. Marker, and A. R. Thomsen. 1996. T-cell mediated immunity to lymphocyte choriomeningitis virus in β_2-integrin (CD18)- and ICAM-1 (CD54)-deficient mice. *J. Virol. 70:8997.*
38. Anderson, E. C., J. P. Christensen, A. Scheynius, O. Marker, and A. R. Thomsen. 1995. Lymphocytic choriomeningitis virus infection is associated with long standing perturbation of LFA-1 expression on $CD8^+$ T cells. *Scand. J. Immunol. 42:110.*
39. Nielsen, H. V., J. P. Christensen, E. C. Andersson, O. Marker, and A. R. Thomsen. 1994. Expression of type 3 complement receptor on activated CD8 T cells facilitate homing to inflammatory sites. *J. Immunol. 153:2021.*
40. Williams, M. B., and E. C. Butcher. 1997. Homing of naïve and memory T lymphocyte subsets to Peyer's patches, lymph nodes and spleen. *J. Immunol. 159:1746.*
41. Mohamedzadeh, M., H. DeGrendele, H. Arizpe, P. Estess, and M. Siegelman. 1998. Proinflammatory stimuli regulate endothelial hyaluronan expression and CD44/HA-dependentt primary adhesion. *J. Clin. Invest. 101:97.*
42. Graesser, D., S. Mahooti, T. Haas, S. Davis, R. B. Clark, and J. A. Madri. 1998. The interrelationship of α_4 integrin and matrix metalloproteinase-2 in the pathogenesis of experimental autoimmune encephalomyelitis. *Lab. Invest. 78:1445.*
43. Rodrigues, M., R. S. Nussenzweig, P. Romero, and F. Zavala. 1992. The in vivo cytotoxic activity of $CD8^+$ T cell clones correlates with their levels of expression of adhesion molecules. *J. Exp. Med. 175:895.*
44. Mazanet, M. M., K, Neote, and C. C. W. Huges. 2000. Expression of IFN-inducible T cell α chemoattractant by human endothelial cells is cyclosporin A-resistant and promotes T cell adhesion: implications for cyclosporin A-resistant immune inflammation. *J. Immunol. 164:5383.*